scientific reports

Check for updates

OPEN

# Transcriptomic analysis of the anti-tumor effects of leflunomide in prolactinoma

Xiangdong Pei, Yuyang Peng, Huachun Yin, Zhenle Zang, Kaifeng Shen, Song Li & Chunqing Zhang✉

**Leflunomide's anti-tumor effects have been investigated in various types of tumors; however, its impact on pituitary adenoma, particularly prolactinoma, is unclear. Hence, the current study evaluates the effects of leflunomide on prolactinoma cells in vitro and in vivo and elucidates the potential underlying mechanism(s). Cell Counting Kit-8 results revealed that leflunomide inhibits the proliferation of rat pituitary tumor cell lines (GH3 and MMQ) in a concentration-dependent manner in vitro. However, combination therapy of cabergoline and leflunomide exerted stronger inhibitory effects than cabergoline in MMQ cells in vitro and in vivo. Transcriptomics and gene ontology (GO) analyses identified genes significantly enriched in apoptotic processes and programmed cell death. Protein–Protein Interaction (PPI) networks defined the roles of hub genes (Mdm2, Cdkn1a, Plk2, and Ccng1) in leflunomide-induced cell death. GO and pathway enrichment analyses showed that the combination drug-specific differentially expressed genes were associated with inhibiting protein translation, but were active in gene expression processes. Hence, the anti-proliferative effects of leflunomide on prolactinoma cell lines may be mediated through programmed cell death pathways. Importantly, combining cabergoline with leflunomide effectively enhances the toxic effect of cabergoline, suggesting a potential therapeutic role for leflunomide in drug-resistant prolactinoma.**

**Keywords** Leflunomide, Prolactinoma, Anti-tumor effect, Transcriptional differences

Prolactinoma comprises 40–45% of all adult functional pituitary adenomas, which can lead to headache, visual dysfunction, hypophysis dysfunction, and hyperprolactinemia[1–3]. Dopamine agonists (e.g., cabergoline and bromocriptine) have been suggested as first-line treatments for prolactinoma, among which cabergoline exhibits high efficacy and elicits few side effects[4,5]. However, the ensemble epidemiology of drug resistance is 20–30% for bromocriptine (BRC) and ~ 10% for cabergoline (CAB) in patients with prolactinoma who have undergone surgery[6]. Therefore, new anti-tumor drug treatment strategies may be important for patients with prolactinoma.

Leflunomide—a dihydroorotate dehydrogenase (DHODH) inhibitor—has obtained approval for treating rheumatoid arthritis[7–10]. Additionally, clinically meaningful remission has been achieved in patients with relapsed glioblastoma following leflunomide treatment[11]. Mechanistically, leflunomide and its active metabolite exhibit anti-tumor effects by reducing proliferation and inducing apoptosis in neuroblastoma and multiple myeloma cells[12,13]. A case series revealed the remarkable therapeutic advantages of leflunomide in addressing myriad malignancies, including medullary thyroid cancer, prostate cancer, lymphoblastic leukemia, breast cancer, leukemia, hepatocellular carcinoma, melanoma, etc[14–24]. Moreover, combining leflunomide and a BRAF inhibitor significantly enhances melanoma growth inhibition[25]. In the past decade, leflunomide has been used in various preclinical studies to assess its potential in treating central nervous system malignancies, neuroblastoma, and prostate cancer[26–28]. However, whether it exerts similar anti-tumor effects on pituitary adenoma, particularly prolactinoma, remains unknown.

In the current study, the effects of leflunomide on prolactinoma cells are investigated in vitro and in vivo. Additionally, the underlying molecular mechanisms are characterized using transcriptomics and bioinformatics analyses.

Department of Neurosurgery, Xinqiao Hospital, Army Medical University, Chongqing 400037, China. ✉email: cqzhang@tmmu.edu.cn

## Materials and methods

### Cell lines

The MMQ (CRL-10609, ATCC) and GH3 (CCL-82.1, ATCC) rat prolactinoma cell lines were acquired from American Type Culture Collection (ATCC, Manassas, VA, USA). They were cultured in a complete medium based on Ham's F-12 K medium (Gibco, 21127-022) with 2.5% fetal bovine serum (FBS; 04-001-1ACS, Biological Industries), 15% horse serum (Gibco, 16050-122), and 1% penicillin/streptomycin. Cells were cultured at 37 °C and 5% CO2. All experiments are performed in accordance with the relevant manufacturer's instructions or guidelines.

### CCK-8 assay

MMQ and GH3 cells were evenly seeded into 96-well plates, with $5 \times 10^3$ or $1 \times 10^4$ cells per well and different concentrations of reagents. Cabergoline (HY-15296) and leflunomide (HY-B0083) were purchased from MedChemExpress and dissolved in dimethyl sulfoxide (DMSO). Cell viability was assessed after 0, 24, 48, and 72 h by measuring the absorbance at 450 nm. Each experiment was conducted in triplicate.

### Xenograft experiments

Female BALB/cA-nu mice of 4-week-old were purchased from Beijing HFK Bioscience Co. Ltd. in China and raised under specific pathogen-free (SPF) conditions. MMQ cells ($4 \times 10^6$) suspended in a solution containing 50% Matrigel (100 µL) were injected into the lateral abdomen of mice. The tumor bearing animals were randomly divided into four groups (9 mice/group). Cabergoline or leflunomide was administered 9 d after inoculation for three weeks until the mice were euthanized by carbon dioxide asphyxiation[29]. The mice were weighed, and their tumor volumes were measured. Tumor volumes were computed as V ($mm^3$) = [$AB^2$]/2, where A denotes the length of the tumor and B indicates the width of the tumor. This study was carried out adhered to the ARRIVE guidelines[30]. All experiments were conducted in accordance with relevant guidelines and regulations, complying with the International Guiding Principles for Biomedical Research Involving Animals[31;32]. All experimental protocols and animal operations were approved by the ethics committee of Army Medical University (code: AMUWEC20210074).

### Transcriptomic analysis

Cells were processed to extract total RNA per the manufacturer's guidelines. The ND-1000 Nanodrop spectrophotometer (NanoDrop Technologies, Wilmington, DE, USA) was used to assess the quantity and quality of the extracted RNA. The integrity of the RNA was assessed using an Agilent 2200 TapeStation (Agilent Technologies, Santa Clara, CA, USA). All samples exhibited a RINe value > 7.0.rRNA was extracted using the Epicenter Ribo-Zero rRNA Removal Kit (Illumina, San Diego, CA, USA) and fragmented into ~ 200 bp segments. RNA was reverse transcribed into cDNA before ligating adaptors and enriching the samples using a low-cycle method following the instructions of the TruSeq® RNA LT/HT Sample Prep Kit (Illumina). The library items were assessed and subsequently subjected to sequencing (2 × 100 bp) using HiSeq 2500.

The libraries underwent analysis through the Illumina HiSeq platform. The SolexaQA package maintained integrity of the initial sequencing data by eliminating reads containing adapters, synthetic sequences, or nucleotides with a quality score < 20[33]. Then, the cleaned sequencing reads were then aligned to the genome using the TopHat BWA software[34].

### Differentially expressed genes (DEGs) selection

Cufflinks (v1.0.3) was used to evaluate the transcriptional levels of each gene[35]. The data were sourced from the UCSC database for the purpose of reference genome annotation. The data were normalized by adjusting for variations in sequencing depth, standardizing to fragments per kilobase of exon per million mapped reads. Subsequently, genes with low or no expression were filtered. DEGs were identified between treated and the R package[36]. Genes with a FC > 2 and *P*-value < 0.05 were classified as DEGs.

### Enrichment mapping and PPI analysis

GO, pathway enrichment, and death-related DEG identification were carried out using the ToppGene and Metascape websites. The findings were considered statistically significant with P-values < 0.05[37,38]. To determine the states of the GO term and pathway under specific conditions, the Z-score values were calculated using Eq. (1):

$$Z - score = \frac{N_{up} - N_{down}}{\sqrt{N_{up} + N_{down}}} \quad (1)$$

where $N_{up}$ represents the number of overexpressed DEGs, and $N_{down}$ indicates the number of underexpressed DEGs.

To investigate the drug-related PPI in MMQ, the differentially expressed genes (DEGs) were correlated with the STRING online database, which has a built-in NetworkAnalyst and Metascape[39]. The InfoMap and MCODE algorithms were utilized to identify the modules within the PPI network, and the results were displayed using Cytoscape.

### Statistical analysis

The data are expressed as mean ± standard error of the mean (SEM). A two-tailed Student's t-test was applied to determine statistical significance between the two groups. These analyses were performed using SPSS for Windows, version 13.0 (SPSS Inc., USA).

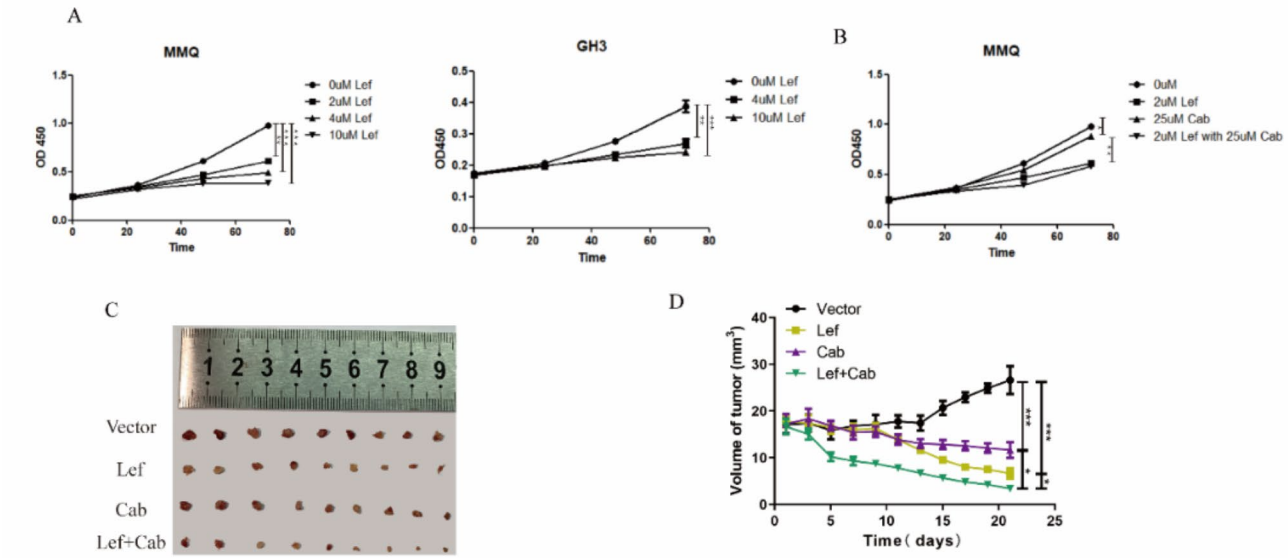


**Fig. 1**. Toxic function of leflunomide on prolactinoma cell lines. (**A**) MMQ and GH3 cells were incubated with different concentration of leflunomide for 0, 24, 48, or 72 h, and cell proliferation was assessed at different time points by a CCK-8 assay ($n = 6$, ± SEM) in each group (GH3: 4 μmol/L Lef vs. 0 μmol/L Lef: $^{**}P = 9.88 \times 10-4 < 0.01$, 10 μmol/L Lef vs. 0 μmol/L Lef: $^{***}P = 5.68 \times 10-5 < 0.001$; MMQ: 2 μmol/L Lef vs. 0 μmol/L Lef: $^{**}P = 7.98 \times 10-8 < 0.01$, 4 μmol/L Lef vs. 0 μmol/L Lef: $^{***}P = 5.40 \times 10-8 < 0.01$, 10 μmol/L Lef vs. 0 μmol/L Lef: $^{***}P = 1.30 \times 10-9 < 0.001$). (**B**) MMQ cells were incubated with/without leflunomide and cabergoline alone or in combination for 0, 24, 48, or 72 h, and cell proliferation was assessed at different time points by a CCK-8 assay ($n = 6$, ± SEM; 25 μmol/L Cab vs. 0 μmol/L: $^{*}P = 0.001527 < 0.05$, 2 μmol/L Lef with 25 μmol/L Cab vs. 0 μmol/L: $^{**}P = 8.32 \times 10-8 < 0.01$). (**C**) Excised tumors in different treatment groups. (**D**) Growth curve showing the changes in the tumor volume in mice after different treatments. (Lef vs. vector: $^{***}P = 1.18 \times 10-5 < 0.001$, Cab vs. vector: $^{***}P = 0.000498 < 0.001$, Lef + Cab vs. Cab: $^{***}P = 0.000241 < 0.001$, Lef + Cab vs. Lef: $^{*}P = 0.002 < 0.05$).

| Gene | Log (FC) | *P*-value | Gene | Log (FC) | *P*-value |
|---|---|---|---|---|---|
| *Mff* | 2.627 | 0.002 | *Nhp2* | − 3.056 | 0.007 |
| *Txnip* | 2.323 | 0.002 | *Stx7* | − 2.425 | 0.042 |
| *Ptprv* | 2.224 | $1.824 \times 10^{-17}$ | *Rmrp* | − 1.723 | $5.2 \times 10^{-5}$ |
| *Phlda3* | 2.081 | $3.622 \times 10^{-29}$ | *Rplp2* | − 1.231 | 0.0003 |
| *Cd80* | 2.015 | $9.068 \times 10^{-6}$ | *Akap5* | − 1.070 | 0.001 |

**Table 1**. Top five differentially expressed genes (DEGs) with up- and down-regulation.

## Results

### Leflunomide exerts toxic effects on prolactinoma cell lines

The impact of leflunomide (Lef) on cell lines derived from prolactinoma was investigated. Cell Counting Kit-8 results revealed that leflunomide inhibited the proliferation of GH3 and MMQ cells in a concentration-dependent manner (Fig. 1A). Specifically, 2 μmol/L, 4 μmol/L, and 10 μmol/L of leflunomide inhibited pituitary tumor MMQ cell growth ($P < 0.05$), while 4 μmol/L and 10 μmol/L inhibited GH3 cells ($P < 0.05$) in a time- and dose-dependent manner.

The combined application of 2 μmol/L leflunomide and 25 μmol/L cabergoline (Cab) elicited significantly enhanced inhibitory effects on MMQ cells than cabergoline alone ($P < 0.05$). Hence, leflunomide may enhance the efficacy of cabergoline (Fig. 1B). In vivo, leflunomide hindered the growth of MMQ cell-derived tumors and enhanced the efficacy of cabergoline (Fig. 1C,D).

### DEGs in MMQ following Leflunomide treatment

To elucidate the mechanism underlying the inhibition of MMQ cells by leflunomide, differentially expressed genes (DEGs) associated with leflunomide treatment were identified. A total of 101 upregulated and 17 downregulated DEGs with a |fold change (FC)|> 2 and P-value < 0.05, were identified (Table S1). Of these, genes associated with cell death regulation (Mff, Txnip, and Phlda3), membrane proteins (Ptprv), and immune co-stimulatory molecules (Cd80) were significantly upregulated (Table 1). Meanwhile, genes associated with rRNA

biogenesis (Nhp2), intracellular trafficking (Stx7), tumors (Rmrp and Rplp2), and neuronal activities (Akap5) were downregulated in cells treated with leflunomide.

Based on the gene ontology (GO) biological process enrichment analysis (Fig. 2A), the top 10 functional terms associated with the DEGs were significantly enriched in the cell death process. The regulation of apoptotic processes and programmed cell death had the highest z-scores (z-score = 4.58, Table S1). However, the negative regulation of cell death, apoptosis, and programmed cell death also had high z-scores (4.24, 4.00, and 4.00, respectively). Other processes also had active trends, such as response to abiotic stimuli (z-score = 2.98), central nervous system development (z-score = 3.58), and response to organonitrogen compounds (z-score = 2.98). Regarding pathway enrichment (Fig. 2B), the p53 signaling pathway with the highest z-score (z-score = 2.45) was significantly activated. An active trend was also observed in viral carcinogenesis, with the second highest z-score (z-score = 2.23). Moreover, the PI3K–AKT signaling pathway, platinum drug resistance, longevity regulating pathway, endocrine resistance, glucagon signaling pathway, FoxO signaling pathway, and cell adhesion molecules exhibited active trends (z-scores > 1).

To investigate the cell death caused by related biological processes in MMQ cells treated with leflunomide, 26 cell death-related genes were identified by GO enrichment between the experimental and control groups (Fig. 2C). Only Hk2 was downregulated in MMQ cells following leflunomide treatment and 25 cell death-related genes, including Cdkn1a, Ccng1, and Plk2, were upregulated.

### PPI network analysis of hub genes following Leflunomide treatment

To clarify how cell death regulation is controlled during leflunomide treatment, DEGs were utilized to construct the protein–protein interactions (PPI) network and modules using the STRING database (Fig. 2D). Nodules were identified based on an adjusted P-value of < 0.05 and degree in modules > 20. According to the degree of each node, upregulated genes Mdm2 with the highest degree regulated 115 genes, Cdkn1a regulated 74 genes, Plk2 regulated 53 genes, and Ccng1 regulated 27 genes. The InfoMap algorithm from the network module was utilized to investigate the functional connections among the DEGs. Two modules were identified with more than 20 community nodes and adjusted P-value < 0.05 (Fig. 2E). The modules in MMQ cells treated with leflunomide exhibited an interactive relationship, with eight nodes regulated by the hub genes Cdkn1a and Ccng1. In the module with the most nodes, cellular senescence and ubiquitin-mediated proteolysis were regulated by Mdm2 upregulation. Additionally, increased Cdkn1a and Ccng1 expression regulated the cell cycle and cellular senescence.

### Significant changes in MMQ cells treated with Cabergoline and combination therapy

To investigate the possibility of PRL tumor inhibition and the mechanistic role of cabergoline and combined cabergoline and leflunomide therapy, DEGs were identified between the control, combined therapy, and cabergoline treatment. There were 268 (202 upregulated and 66 downregulated) DEGs identified in the cabergoline-treatment group (Fig. 3A). These genes were significantly associated with positive regulation of cell death processes and the apoptotic signaling pathway (Fig. 3B). Moreover, they are crucial in dysfunctional metabolic processes, including steroid biosynthesis and monocarboxylic acid metabolism. Module analysis revealed two main modules in the PPI network (Fig. 3C). MCODE 1 is associated with amino acids regulating mTORC1. MCODE 2 is associated with collagen fibril structure assembly. Meanwhile, the transcription factor SP1 was predicted to regulate 15 DEGs in cabergoline treatment, with most genes playing a key role in controlling apoptosis and cell cycle functions (Fig. 3D).

Next, we investigated the fundamental mechanisms through which leflunomide boosts the anti-cancer properties of cabergoline. Thirteen DEGs, including Rplp2, Tprkb, and Hnrnpab, were detected between the combination treatment and cabergoline groups (Fig. 3E). Compared with the cabergoline group, eight genes were downregulated (Mrpl53, Cttn, Snrpg, Iars1, Mir1956, Mir25, Hnrnpc, and U5) and five genes were upregulated (Loc688583, Rplp2, Tprkb, hnrnpab, and Vps50) in the combination treatment group. GO and pathway enrichment analyses showed that the combination drug-specific DEGs were predominantly enriched in protein translation inhibition, but were active in gene expression processes, such as ribonucleoprotein complex, protein-containing complex binding, and translation (Fig. 3F). In particular, Rplp2 and hnrnpab played important roles in inhibiting translation.

## Discussion

Leflunomide can effectively block the function of DHODH, a crucial enzyme in the de novo biosynthesis of pyrimidine, and plays a significant role in cell survival[40]. In the current study, we found that leflunomide effectively inhibited the proliferation of prolactinoma cell lines and enhanced the toxic effect of cabergoline in vitro and in vivo. In the cells subjected to leflunomide treatment, 101 genes were identified as upregulated, whereas 17 genes were downregulated. The top five upregulated genes were associated with cell death regulation molecules, membrane molecules, and immune-associated. The downregulated genes were related to immunity, intracellular trafficking, tumors, and neuronal activity. Further transcriptomic analyses revealed the underlying mechanisms associated with the programmed cell death pathway in cells treated with leflunomide. The hub genes Cdkn1a, Ccng1, and Mdm2 regulated cellular senescence and cell cycle processes. Additionally, DEGs from cells treated with cabergoline significantly enriched in positive regulation of cell death processes and apoptotic signaling pathways. The transcription factor SP1 in cabergoline-treated cells regulates 15 genes with key roles in controlling apoptosis and cell cycle functions. Furthermore, 13 DEGs were detected in combination therapy-treated cells. The inhibition of the translation process was significantly enriched in cells treated with the combined drugs compared with cabergoline.

The anti-tumor effects of leflunomide have been reported in various cancers. Zhu et al. reported that leflunomide inhibits neuroblastoma cell growth and promotes cell death in vitro and in vivo[13]. Moreover,

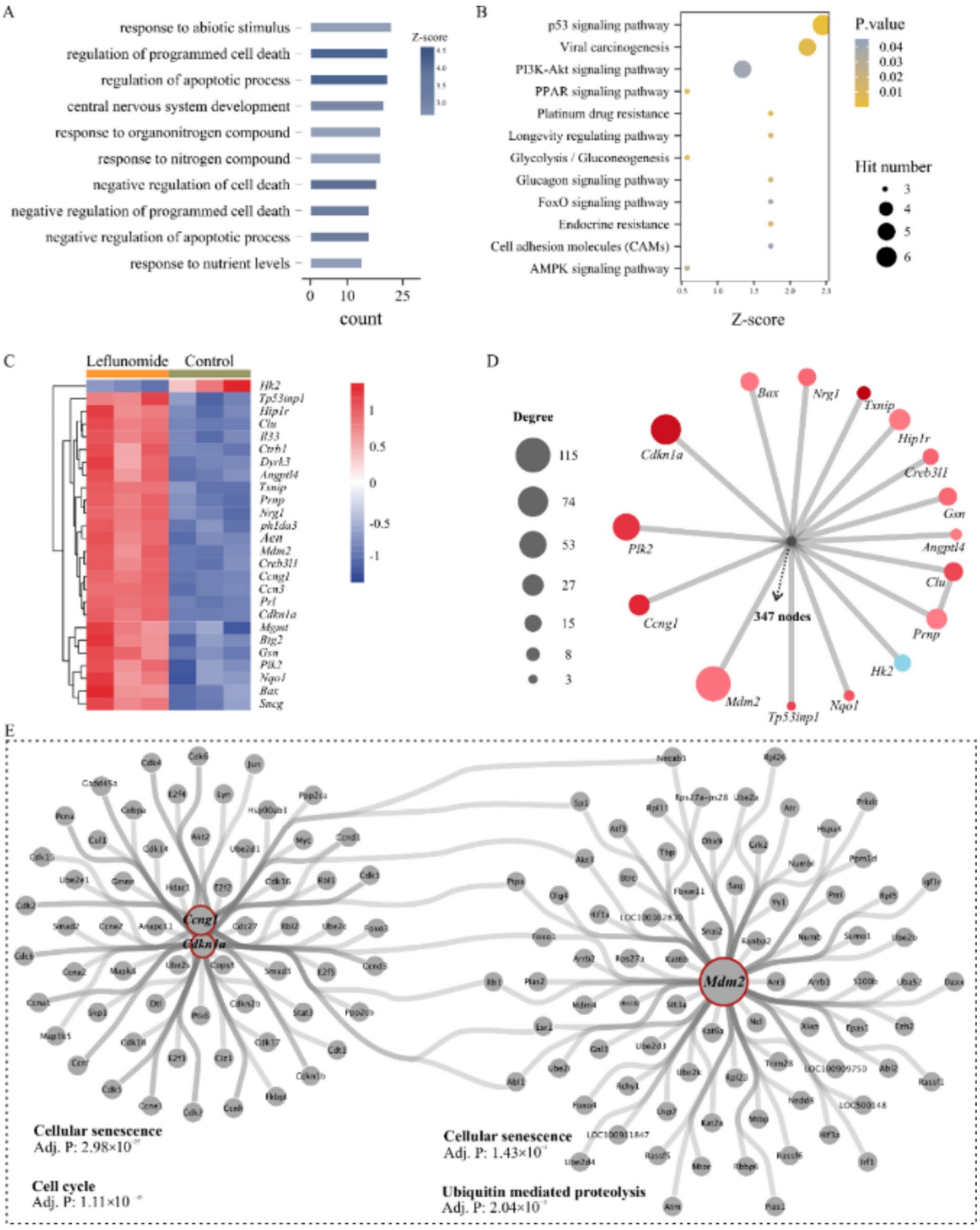


**Fig. 2**. Function of death-related differentially expressed genes (DEGs) in leflunomide. (**A**) Gene Ontology (GO) enrichment of DEGs. (**B**) Pathway enrichment of DEGs. (**C**) Heatmap of death-related DEGs. (**D**) Protein–Protein Interaction (PPI) development networks of death-related DEGs; circles represent genes; color intensity: fold change level; red: upregulated DEGs; blue: downregulated DEGs; overlapping nodes: 347 genes. (**E**) Module analysis; red: upregulated genes.

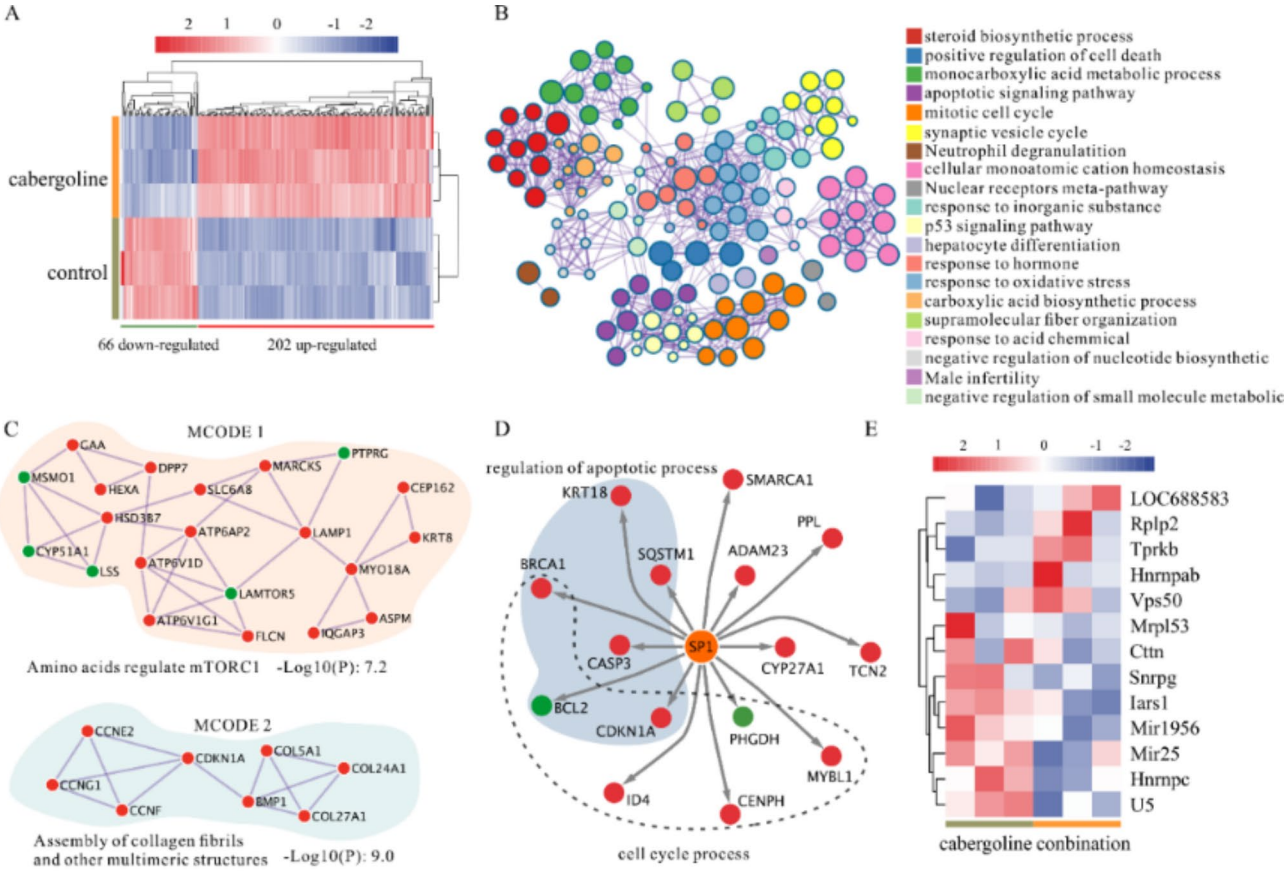


F

| Category | Name | P value | Gene | Z score |
|---|---|---|---|---|
| GO: Cellular Component | ribonucleoprotein complex | $7.32\times10^{-5}$ | Mir25, Rplp2, Snrpg, Hnrnpab, Mrpl53 | -0.45 |
| Pathway | gene expression | 0.014 | Rplp2, Snrpg, Iars1,Tprkb | 0 |
| GO: Molecular Function | protein-containing complex binding | 0.036 | Cttn, Snrpg, Hnrnpab | -0.58 |
| GO: Biological Process | RNA modification | $5.48\times10^{-5}$ | Snrpg, Hnrnpab,Tprkb | 0.58 |
| GO: Biological Process | translation | 0.005 | Rplp2, Mrpl53, Iars1 | -0.58 |
| GO: Cellular Component | synapse | 0.030 | Cttn, Snrpg, Hnrnpab | -0.58 |
| GO: Cellular Component | catalytic complex | 0.037 | Snrpg, Hnrnpab, Iars1 | -0.58 |

**Fig. 3**. Functional role of important differentially expressed genes (DEGs) associated with cabergoline and combination drugs. (**A**) Heatmap of DEGs in cabergoline. (**B**) Gene Ontology (GO) and pathway enrichment of DEGs related to cabergoline use; nodes: enrichment terms; terms ranked by significant *P*-values. (**C**) Module analysis of the Protein–Protein Interaction (PPI) network created with Metascape (https://metascape.org/gp/index.html#/main/step1). (**D**) Transcription factor (TF)-regulated network in cabergoline; red nodes: up-regulated DEGs, green nodes: down-regulated genes. (E) DEGs between cabergoline combined drugs. (**F**) GO and pathway enrichment of DEGs between cabergoline and combined drugs.

leflunomide evokes anti-angiogenic and anti-proliferative activities in Ehrlich-Lettre ascites carcinoma cells in vivo[15]. Similarly, in the current study, treating MMQ cells with different concentrations of leflunomide exerted inhibitory effects in vitro and in vivo, confirming the potential therapeutic role of leflunomide in prolactinoma.

Additionally, we examined the expression levels of the 26 cell death-related genes identified by GO enrichment. Accordingly, most cell death-related genes, excluding *Hk2*, were upregulated under leflunomide treatment; *Mff*, *Txnip*, and *Phlda3* were among the top five DEGs. Furthermore, PPI network analysis identified two communities and three hub genes. Cell senescence and cell cycle were enriched in community functions, suggesting that apoptosis was the main mechanism by which leflunomide inhibited the proliferation of prolactinoma cells. Leflunomide significantly reduces the cell viability of bladder cancer cells by inducing apoptosis and cell cycle arrest and suppressing the PI3K/AKT signaling pathway[41]. Similarly, leflunomide induces apoptosis of HeLa cells. Moreover, leflunomide-induced inhibition of DHODH reduces phosphorylation of AKT, p70S6K, and 4E-binding protein-1, and alters the expression of BCL-2 family proteins[42]. These studies align with our findings and confirm that apoptosis plays a vital role in the death of MMQ cells induced by leflunomide.

Combinatorial treatment with leflunomide and other chemopreventive drugs, such as gemcitabine, fludarabine, selumetinib, and oxaliplatin have strong beneficial effects in treating pancreatic cancer, hepatocellular

carcinoma, chronic lymphocytic leukemia, small cell lung cancer, and melanoma cells in vitro[19,43–45]. Moreover, leflunomide regulates the drug resistance of breast cancer drug-resistant protein (BCRP) and antagonizes the induced proliferation of CD40L/IL4 at very low concentrations to overcome the apoptosis resistance of CLL cells[18,19]. Meanwhile, we have shown that combining leflunomide and the dopamine agonist cabergoline enhances the inhibitory effect of cabergoline on MMQ cells. The DEGs between the combined group and single cabergoline group were predominantly associated with the translation inhibition process. Dietrich et al. found that leflunomide inhibit CD40L-induced fludarabine resistance by affecting both JAK/STAT and NF-κB signaling that leads to reduced BCL-XL and MCL1 expression, which is consistent with our transcriptomic findings of leflunomide. Furthermore, similar to our results, leflunomide reportedly blocks the effect of UBE2T by promoting AKT K63-linked ubiquitination and enhanced selumetinib's inhibition on triple-negative breast cancer's growth by suppressing pyrimidine synthesis increases which in response to genotoxic stress[46,47].

## Data availability

The datasets generated and analysed during the current study are available in the SRA repository (https://www.ncbi.nlm.nih.gov/bioproject/PRJNA1196593).

Received: 5 December 2024; Accepted: 21 March 2025
Published online: 05 April 2025

## References

1. Haidenberg-David, F. et al. Overview of hyperprolactinemia: general approach and reproductive health implications. *Arch. Med. Res.* **55**, 103102 (2024).
2. Tang, H. et al. Drd2 expression based on 18F-Fallypride Pet/Mr predicts the dopamine agonist resistance of prolactinomas: A pilot study. *Endocrine* **80**, 419–424 (2023).
3. Glezer, A., Santana, M. R., Bronstein, M. D., Donato, J. J. & Jallad, R. S. The interplay between prolactin and cardiovascular disease. *Front. Endocrinol.* **13**, 1018090 (2022).
4. Shimon, I. Real-World value of Cabergoline in the treatment of acromegaly. *Best Pract. Res. Clin. Endocrinol. Metab.* **38**, 101887 (2024).
5. Fachi, M. M., de Deus Bueno, L., de Oliveira, D. C., da Silva, L. L. & Bonetti, A. F. Efficacy and safety in the treatment of hyperprolactinemia: A systematic review and network Meta-analysis. *J. Clin. Pharm. Ther.* **46**, 1549–1556 (2021).
6. Maiter, D. Management of dopamine Agonist-Resistant prolactinoma. *Neuroendocrinology* **109**, 42–50 (2019).
7. Boharoon, H. & Grossman, A. A. New medical therapy for multiple endocrine neoplasia type 1? *TouchREV Endocrinol.* **18**, 86–88 (2022).
8. Kim, S. et al. Pembrolizumab-Induced psoriatic arthritis treated with Disease-Modifying Anti-rheumatic drugs in a patient with gastric cancer: A case report. *World J. Clin. Cases*. **11**, 218–224 (2023).
9. Peretti, S. et al. The Yin-Yang pharmacomicrobiomics on treatment response in inflammatory arthritides: A narrative review. *Genes (Basel)*. **14**, 89 (2022).
10. Salazar, D. M. et al. Leflunomide-Induced Immune-Mediated necrotizing myopathy in a patient with rheumatoid arthritis: A case report. *J. Investig Med. High. Impact Case Rep.* **11**, 23247096221150636 (2023).
11. Castro, M. P. et al. Targeting chromosome 12Q amplification in relapsed glioblastoma: the use of computational biological modeling to identify effective therapy-A case report. *Ann. Transl Med.* **10**, 1289 (2022).
12. Baumann, P. et al. Dihydroorotate dehydrogenase inhibitor a771726 (Leflunomide) induces apoptosis and diminishes proliferation of multiple myeloma cells. *Mol. Cancer Ther.* **8**, 366–375 (2009).
13. Zhu, S., Yan, X., Xiang, Z., Ding, H. F. & Cui, H. Leflunomide reduces proliferation and induces apoptosis in neuroblastoma cells in vitro and in vivo. *Plos One*. **8**, e71555 (2013).
14. Hwang, C. & Heath, E. I. Angiogenesis inhibitors in the treatment of prostate cancer. *J. Hematol. Oncol.* **3**, 26 (2010).
15. Bahr, H. I. et al. Chemopreventive effect of Leflunomide against Ehrlich's solid tumor grown in mice: effect on Egf and EGFR expression and tumor proliferation. *Life Sci.* **141**, 193–201 (2015).
16. Uckun, F. M. Chemosensitizing Anti-cancer activity of Lfm-a13, a Leflunomide metabolite analog targeting Polo-Like kinases. *Cell. Cycle*. **6**, 3021–3026 (2007).
17. Doscas, M. E. et al. Inhibition of P70 S6 kinase (S6K1) activity by a77 1726 and its effect on cell proliferation and cell cycle progress. *Neoplasia* **16**, 824–834 (2014).
18. Kis, E. et al. Leflunomide and its metabolite a771726 are high affinity substrates of Bcrp: implications for drug resistance. *Ann. Rheum. Dis.* **68**, 1201–1207 (2009).
19. Dietrich, S. et al. Leflunomide induces apoptosis in Fludarabine-Resistant and clinically refractory Cll cells. *Clin. Cancer Res.* **18**, 417–431 (2012).
20. Alhefdhi, A., Burke, J. F., Redlich, A., Kunnimalaiyaan, M. & Chen, H. Leflunomide suppresses growth in human medullary thyroid cancer cells. *J. Surg. Res.* **185**, 212–216 (2013).
21. Nasr, M., Selima, E., Hamed, O. & Kazem, A. Targeting different angiogenic pathways with combination of Curcumin, Leflunomide and Perindopril inhibits Diethylnitrosamine-Induced hepatocellular carcinoma in mice. *Eur. J. Pharmacol.* **723**, 267–275 (2014).
22. Hailm N. J., Chen, P. & Bushman, L. R. Teriflunomide (Leflunomide) promotes cytostatic, antioxidant, and apoptotic effects in transformed prostate epithelial cells: evidence supporting a role for Teriflunomide in prostate cancer chemoprevention. *Neoplasia* **12**, 464–475 (2010).
23. O'Donnell, E. F. et al. The Aryl hydrocarbon receptor mediates Leflunomide-Induced growth Inhibition of melanoma cells. *Plos One*. **7**, e40926 (2012).
24. Ringshausen, I., Oelsner, M., Bogner, C., Peschel, C. & Decker, T. The Immunomodulatory drug Leflunomide inhibits cell cycle progression of B-Cll cells. *Leukemia* **22**, 635–638 (2008).
25. White, R. M. et al. Dhodh modulates transcriptional elongation in the neural crest and melanoma. *Nature* **471**, 518–522 (2011).
26. Adamson, P. C. et al. Pediatric phase I trial and Pharmacokinetic study of the Platelet-Derived growth factor (Pdgf) receptor pathway inhibitor Su101. *Cancer Chemother. Pharmacol.* **53**, 482–488 (2004).
27. Ko, Y. J. et al. A Multi-institutional phase Ii study of Su101, a Platelet-Derived growth factor receptor inhibitor, for patients with Hormone-Refractory prostate cancer. *Clin. Cancer Res.* **7**, 800–805 (2001).
28. Eckhardt, S. G. et al. Phase I and Pharmacologic study of the tyrosine kinase inhibitor Su101 in patients with advanced solid tumors. *J. Clin. Oncol.* **17**, 1095–1104 (1999).
29. Alejo, A. L. et al. A Pre-Clinical standard operating procedure for evaluating orthobiologics in an in vivo rat spinal fusion model. *J. Orthop. Sports Med.* **4**, 224–240 (2022).

30. McGrath, J. C., Drummond, G. B., McLachlan, E. M., Kilkenny, C. & Wainwright, C. L. Guidelines for reporting experiments involving animals: the arrive guidelines. *Br. J. Pharmacol.* **160**, 1573–1576 (2010).
31. International Guiding Principles for Biomedical Research Involving Animals Issued by Cioms. *Vet. Q.* **8**, 350–352 (1986).
32. Brown, M. J. et al. *Cult. Care: Organizational Responsibilities* 11–26 (2018).
33. Cox, M. P., Peterson, D. A., Biggs, P. J. & Solexaqa At-a-Glance quality assessment of illumina Second-Generation sequencing data. *BMC Bioinform.* **11**, 485 (2010).
34. Trapnell, C., Pachter, L. & Salzberg, S. L. Tophat: discovering splice junctions with Rna-Seq. *Bioinformatics* **25**, 1105–1111 (2009).
35. Trapnell, C. et al. Differential gene and transcript expression analysis of Rna-Seq experiments with tophat and cufflinks. *Nat. Protoc.* **7**, 562–578 (2012).
36. Robinson, M. D., McCarthy, D. J., Smyth, G. K. & Edger A bioconductor package for differential expression analysis of digital gene expression data. *Bioinformatics* **26**, 139–140 (2010).
37. Zhou, Y. et al. Metascape provides a Biologist-Oriented resource for the analysis of Systems-Level datasets. *Nat. Commun.* **10**, 1523 (2019a).
38. Chen, J., Bardes, E. E., Aronow, B. J. & Jegga, A. G. Toppgene suite for gene list enrichment analysis and candidate gene prioritization. *Nucleic Acids Res.* **37**, W305–W311 (2009).
39. Zhou, G. et al. Networkanalyst 3.0: A visual analytics platform for comprehensive gene expression profiling and Meta-analysis. *Nucleic Acids Res.* **47**, W234–W241 (2019b).
40. Zhang, C., Chu, M. & Leflunomide A promising drug with good antitumor potential. *Biochem. Biophys. Res. Commun.* **496**, 726–730 (2018).
41. Cheng, L. et al. Leflunomide inhibits proliferation and induces apoptosis via suppressing autophagy and Pi3K/Akt signaling pathway in human bladder cancer cells. *Drug Des. Dev. Ther.* **14**, 1897–1908 (2020).
42. Jin, R. et al. Leflunomide suppresses the growth of LKB1-Inactivated tumors in the Immune-Competent host and attenuates distant cancer metastasis. *Mol. Cancer Ther.* **20**, 274–283 (2021).
43. Hanson, K. et al. The Anti-Rheumatic drug, Leflunomide, synergizes with Mek Inhibition to suppress melanoma growth. *Oncotarget* **9**, 3815–3829 (2018).
44. Buettner, R. et al. Leflunomide synergizes with gemcitabine in growth Inhibition of Pc cells and impairs C-Myc signaling through Pim kinase targeting. *Mol. Ther. -Oncolytics.* **14**, 149–158 (2019).
45. Mirzapoiazova, T. et al. Teriflunomide/Leflunomide synergize with chemotherapeutics by decreasing mitochondrial fragmentation via Drp1 in Sclc. *Iscience* **27**, 110132 (2024).
46. Zhu, Z. et al. Ube2T-Mediated Akt ubiquitination and Akt/Beta-Catenin activation promotes hepatocellular carcinoma development by increasing pyrimidine metabolism. *Cell. Death Dis.* **13**, 154 (2022).
47. Brown, K. K., Spinelli, J. B., Asara, J. M. & Toker, A. Adaptive reprogramming of de Novo pyrimidine synthesis is a metabolic vulnerability in Triple-Negative breast cancer. *Cancer Discov.* **7**, 391–399 (2017).


## Author contributions

CQZ designed the research study. XDP and YYP performed the research. YYP, KFS and ZLZ provided help and advice on materials. HCY analyzed the data. SL supervised the project. XDP, HCY, YYP and SL wrote the manuscript. All authors contributed to editorial changes in the manuscript. All authors read and approved the final manuscript.

## Funding

This study was supported by grants from the Natural Science Foundation of Chongqing, China (CSTB2024N-SCQ-MSX0021, CSTB2023NSCQMSX0216), Project for Young and Middle-aged Medical Talents of Chongqing (2024GDRC013) and Young Doctoral Project of Xinqiao Hospital(2022YQB005,2022YQB046).

## Declarations

## Competing interests

The authors declare no competing interests.

## Ethics statement

This study was reviewed and approved by the ethics committee of Army Medical University (AMUWEC20210074). All animal experiments were performed in accordance with the ARRIVE guidelines. All participants have signed informed consent forms.

## Additional information

**Supplementary Information** The online version contains supplementary material available at https://doi.org/10.1038/s41598-025-95509-6.

**Correspondence** and requests for materials should be addressed to C.Z.